

Element stoichiometries of individual plankton cells collected during the Southern Ocean Iron Experiment (SOFeX)

Benjamin S. Twining^{1,2} and *Stephen B. Baines*

Marine Sciences Research Center, Stony Brook University, Stony Brook, New York 11794-5000

Nicholas S. Fisher

Marine Sciences Research Center, Stony Brook University, Stony Brook, New York 11794-5000; and Center for Environmental Molecular Science, Stony Brook University, Stony Brook, New York 11794-5000

Abstract

During the Southern Ocean Iron Experiment (SOFeX), we analyzed Si, P, S, Mn, Ni, and Zn in individual diatoms, autotrophic flagellates, and heterotrophic flagellates with synchrotron-based X-ray fluorescence (SXRF) and calculated cellular C from measurements of cell size. Element stoichiometries for the different types of protists (normalized to either C, S, or P) were generally in good agreement with prior bulk analyses of natural assemblages but also revealed previously undocumented differences in elemental composition among cell types. Flagellated cells contained 39% more P than diatoms, which in turn contained 79% more Mn, 3-fold more Ni, and 2.6-fold more Zn than flagellates. Heterotroph cells contained approximately 40% more P and twice as much Zn as autotrophs. Manganese and Ni stoichiometries were negatively related to cell volume, while larger cells contained more Zn per mole C. Iron fertilization resulted in an approximate doubling of Mn, Ni, and Zn quotas and smaller increases in cellular P, but the timing of the stoichiometric changes varied between the two patches. Silicon contents of diatoms dropped approximately 40% after the first Fe addition but returned to prefertilization levels as cellular P doubled following the second addition, resulting in 40% lower Si:P ratios in the fertilized waters. The mean elemental stoichiometries calculated for all cells analyzed were comparable with previously published extended Redfield ratios for mixed plankton assemblages, but the observed differences between diatoms and flagellates and between autotrophs and heterotrophs indicate that valuable information is lost when all types of co-occurring plankton are grouped together for analysis.

Metal biogeochemistry and ocean ecosystem function are closely linked. Several transition metals, including Mn, Fe, Co, Ni, Cu, and Zn, are required as cofactors for common proteins, and both heterotrophic and autotrophic protists accumulate these elements from the surrounding seawater, lowering dissolved concentrations in surface waters. Remineralization of these metals from sinking cells or zooplankton fecal pellets elevates their concentrations below the euphotic zone, resulting in the nutrient-like profiles commonly observed for these bioactive metals. Further, the availability and accumulation of trace metals can exert control over the biological functioning of the organisms. The availability of

Fe has been shown to limit the growth of heterotrophic bacteria and phytoplankton in high nutrient–low chlorophyll (HNLC) regions (Coale et al. 1996; Pakulski et al. 1996) and certain coastal waters (Hutchins and Bruland 1998). It has been suggested that other metals, such as Zn and Co, could potentially limit the growth of certain phytoplankton species in open ocean environments (Morel et al. 1994; Saito et al. 2002). Thus, the accumulation of metals by plankton can strongly influence the cycling of C in the oceans via the biological pump.

Since Redfield's seminal publications relating elemental stoichiometries of plankton with that of seawater (Redfield et al. 1963), there has been great interest in understanding the relationship between the composition of living organisms and that of their surroundings. Elemental ratios have been used extensively over the years to infer N or P limitation in different waters and to understand the influence of plankton on the elemental composition of seawater. Since the application of trace-metal clean techniques in sampling and analyses started producing meaningful and consistent measurements of metals in water and biota, it has been proposed that an extended Redfield ratio for phytoplankton could be developed that included trace elements (Morel and Hudson 1985). A few painstaking studies directly measured the elemental composition of field-collected plankton assemblages (Martin and Knauer 1973; Martin et al. 1976; Collier and Edmond 1984). While these data are valuable and virtually unique, their interpretation is complicated by the presence of co-occurring particles in the same size range (both living

¹ Corresponding author (benjamin.twining@yale.edu).

² Present address: Yale Institute for Biospheric Studies, P.O. Box 208105, New Haven, Connecticut 06520.

Acknowledgments

The authors gratefully acknowledge Michael Landry for providing the opportunity to participate in the SOFeX project and Chief Scientist Ken Johnson and the Captain and crew of the *R/V Roger Revelle* for enabling the collection of the samples. Jörg Maser, Stefan Vogt, and Dan Legnini provided invaluable technical assistance with the SXRF microprobe, and the manuscript benefited from discussions with Mark Brzezinski and the comments of two anonymous reviewers. Use of the Advanced Photon Source was supported by the U.S. Department of Energy, Office of Science, Office of Basic Energy Sciences, under Contract No. W-31-109-Eng-38. This work was supported by National Science Foundation grants OPP-9986069 and CHE-0221934 and Hudson River Foundation grant 01199A. This is MSRC Contribution No. 1279.

Table 1. Station timing and least-squares mean element ratios for each station as estimated by the ANCOVA model. The year day is presented as a numbered day beginning with 01 January 2002 and is relative to GMT. The station day is relative to the beginning of the first fertilization of each patch. The least-squares mean corrects for differences in the distribution of cell taxa at each station but does not account for differences in the cell-volume distributions at each station (i.e., the model does not assume that the cells are the same size at each station).

Station	North patch				South patch			
	Pre	Fe-1	Fe-2	Out	Pre	Fe-1	Fe-2	Out
Year day	12.0	15.8	18.7	19.5	23.6	27.7	31.0	33.4
Station day	-0.6	3.2	6.2	6.9	-0.7	3.3	6.7	9.3
P:C [†]	19	26	19	21	13	11	24	16
S:C [†]	12	15	10	13	8	7	12	9
Mn:C [‡]	2.5	3.4	5.6	1.8	3.7	2.7	6.0	3.1
Ni:C [‡]	1.8	3.3	5.0	3.6	8.6	5.9	9.2	6.2
Zn:C [‡]	23	23	34	23	45	47	157	88

[†] mmol mol⁻¹.

[‡] μmol mol⁻¹.

and abiotic), as the authors pointed out. Developing an extended Redfield-type ratio using these data is therefore problematic. Moreover, the sensitivity of standard analytical instruments requires plankton to be filtered from large volumes of water. While the resulting stoichiometries may adequately integrate the stoichiometry of the entire plankton community, they provide no information on the composition of individual taxa or cells in the assemblage. Therefore, it is not possible to compare metal accumulation by functionally different cells, such as autotrophs and heterotrophs or naked and ballasted cells (those having dense mineral cell walls).

Laboratory phytoplankton cultures have also been used to study the elemental composition of plankton. In particular, two recent studies present clear taxonomic distinctions in trace-metal stoichiometries (Ho et al. 2003; Quigg et al. 2003). However the applicability of laboratory cultures to natural waters is uncertain because experimental conditions and the composition of the culture media used may not match that of natural waters. Cellular metal quotas are sensitive to light (Sunda and Huntsman 1997), *p*CO₂ (Cullen et al. 1999), and, most importantly, to the chemistry of the ambient water. For metals, culture studies generally attempt to replicate the unchelated trace-metal concentrations of natural waters (Sunda and Huntsman 1998), as this form is generally believed to be most available for organisms. However, recent evidence indicates that phytoplankton may also be able to access metals bound to some ligands (Hutchins et al. 1999; Maldonado and Price 1999; Saito et al. 2002), further complicating the application of culture data to natural systems.

Recently, the development of a new method to measure, accurately and precisely, the trace-element composition of individual phytoplankton and protozoa cells collected from natural waters has made it possible for the first time to assess the elemental composition of different species of co-occurring protist cells (Twining et al. 2003). This method uses a synchrotron-based X-ray fluorescence (SXRF) microprobe to measure Si, P, S, Fe, Mn, Ni, and Zn in individual cells greater than approximately 2 μm in size. The limit of detection of these elements is sufficiently low to allow elemental measurements in cells from virtually all natural waters (Twining et al. 2003). This technique therefore enables

a comparison of the elemental composition of different types of protist cells, including different autotrophic and heterotrophic cells of comparable size, in natural waters. It further enables the separation of living and abiotic particles in the same water sample.

In this study, we applied the unique analytical capabilities of the SXRF microprobe to determine the P, S, Si, Mn, Ni, and Zn stoichiometries of individual plankton cells collected from the mixed layer of the Southern Ocean during the Southern Ocean Iron Experiment (SOFeX). The Fe contents of each target cell were also measured with SXRF and are presented separately elsewhere (Twining et al. in press). By analyzing the elemental composition of individual cells, we can compare the stoichiometries of functionally diverse cells that overlap in size and would, therefore, typically be grouped together during bulk particle analyses. Specifically, we compare the composition of diatoms, ballasted cells with mineral cell walls likely to contribute to vertical C flux, and autotrophic and heterotrophic flagellated cells. These are some of the first measurements of Mn, Ni, and Zn in individual phytoplankton and protozoa cells collected from natural waters.

Materials and methods

A full description of the SOFeX program is given by Coale et al. (2004). Two 15 km × 15 km patches of water in the Pacific sector of the Southern Ocean were fertilized multiple times with ~1 nmol L⁻¹ Fe SO₄. While both patches had high nitrate and phosphate, the patches differed in their Si concentrations. The patch located north of the Antarctic Polar Front Zone (APFZ; North Patch: 56°S, 172°W) contained low concentrations of silicate (3 μmol L⁻¹) and water south of the APFZ (South Patch: 66°S, 172°W) was characterized by high levels of silicate (60 μmol L⁻¹). Plankton samples were collected from each patch prior to the first addition of Fe (Pre stations), following each of the first two fertilizations (Fe-1 and Fe-2 stations), and from stations outside of each patch following the second fertilization (Out stations) for an additional sample of plankton in unfertilized waters. The timing of each station, relative to both GMT and the initial patch fertilizations, is given in Table 1.

Table 2. Volume-normalized concentrations ($\mu\text{mol L}^{-1}$) of Mn, Fe, Ni, and Zn in diatoms, autotrophic flagellates (A flag), and heterotrophic flagellates (H flag) collected from the Southern Ocean prior to Fe fertilization (Low Fe) and following Fe fertilization (High Fe). Mean metal concentrations ($\pm\text{SE}$) are presented for each cell type, as well as for all cells combined.

	Diatoms	<i>n</i>	A flag	<i>n</i>	H flag	<i>n</i>	All cell types	<i>n</i>
Low Fe								
Mn	28 \pm 4	14	48 \pm 10	22	51 \pm 8	28	43 \pm 5	62
Fe	45 \pm 7	16	143 \pm 15	30	270 \pm 50	35	181 \pm 24	80
Ni	98 \pm 24	18	91 \pm 32	22	127 \pm 35	28	77 \pm 9	62
Zn	982 \pm 235	22	455 \pm 74	33	1615 \pm 484	36	1030 \pm 209	90
High Fe								
Mn	48 \pm 8	26	77 \pm 11	40	99 \pm 18	33	68 \pm 6	95
Fe	235 \pm 27	38	715 \pm 94	64	463 \pm 57	65	510 \pm 45	166
Ni	86 \pm 10	36	93 \pm 20	26	104 \pm 16	42	92 \pm 8	101
Zn	1331 \pm 350	41	971 \pm 265	66	2410 \pm 643	69	1418 \pm 190	173

Cells were prepared for SXRF analysis following the protocols of Twining et al. (2003). Briefly, whole water was collected from a plastic-coated rosette used to collect samples for bulk trace-metal analyses. Cells were fixed with glutaraldehyde previously stripped of metal contaminants. Cells were then immediately centrifuged onto gold electron microscopy (EM) grids that were subsequently rinsed with Milli-Q deionized water before drying in a darkened Class-100 hood. Mounted cells were identified with light and epifluorescence microscopy and stored in a desiccator until analysis.

The Si, P, S, Mn, Ni, and Zn contents of the cells were measured with SXRF using the 2-ID-E microprobe at the Advanced Photon Source, Argonne National Laboratory, Argonne, Illinois (Twining et al. 2003). Scan parameters were adjusted for each cell, with pixel step size and dwell time ranging from 0.5 to 1 μm and 1 to 8 s, respectively. X-ray fluorescence spectra from the cell were averaged and fit with a summed exponentially modified Gaussian peak model. Peak areas were corrected for background fluorescence from the C/Formvar film and converted to element concentrations with NIST thin-film standards (NBS 1832, 1833). Because these standards do not contain P, S, or Ni, alternate approaches were taken to quantify these elements. A standard conversion factor for Ni was calculated from a regression of the other element conversion factors on emission energy (r^2 : 0.94–0.98). Phosphorus and S conversion factors were calculated from the Ca conversion factor using P:Ca and S:Ca ratios measured for CaHPO_4 and CaSO_4 standards. These standards enable P and S to be calculated with a precision of 6–8%. Although appropriate plankton reference materials are not available, the accuracy of this technique has been verified through comparative analyses of cultured phytoplankton with SXRF and atomic absorption spectrometry (Twining et al. 2003). Cellular C was estimated for each cell from cell biovolume (BV), which was calculated from linear measurements of each cell using digital micrographs and ImagePro Plus software. The power equations of Menden-Deuer and Lessard (2000) were used to calculate cellular C from BV. While element concentrations are occasionally reported for laboratory cultures, it is difficult to measure the volumes of protist cells in the field, so the elemental contents of plankton are generally normalized to other elements mea-

sured simultaneously. Following this convention, all elements have been normalized to the cellular constituents C, S, or P.

All continuous parameters required log transformation prior to statistical analysis to stabilize variance; outliers were identified and removed on the basis of jackknifed Mahalanobis distances (>2.5 defined as outliers; JMP software, SAS Institute). An analysis of covariance (ANCOVA) model was used to test for statistically significant effects on cell element ratios of the class variables (with group levels) chlorophyll *a* (Chl *a*) (yes/no), station type (Pre/Fe-1/Fe-2/Out), and, for the South patch, cell type (flagellate/diatom). The flagellate group included both dinoflagellates and other unidentified flagellated cells. Cell BV was included as the continuous variable because differences in mean cell size might obscure differences in cell element ratios among the groups. Preliminary analyses indicated that the slope of the relationship between BV and cell element ratio did not differ among groups. Consequently, a single overall slope was used for this relationship in the ANCOVA. Significance of each effect was determined by *F*-tests using Type II sums of squares. The ANCOVA model accounts for differences in the populations of cells at each station, allowing differences between cell types common to all stations, as well as differences between stations in each cell type, to be detected. As presented in Tables 3–5, the influence of BV is indicated by the slope of the linear regression of the element ratio on BV. The influence of the class variables is described by the ratio of the untransformed mean element stoichiometry in one group of cells divided by that in another, so that a value of 1 indicates no difference between groups. For cell types, the elemental ratios for diatoms were divided by those for flagellates, and the ratios for heterotrophs were divided by those for autotrophs.

SXRF provides two-dimensional maps of the element distributions in each cell. While the pixels covering the cell can be summed to provide whole-cell element concentrations, as described above, the maps provide information about the localization of the elements with respect to each other. Additionally, the SXRF element maps can be compared with light and epifluorescence micrographs to determine colocalization of elements with organelles such as chloroplasts.

Table 3. Relative effects of cell volume, Fe addition, cell type, and cell trophic status on cellular S:C, P:C, and P:S in the North and South patches as determined by ANCOVA analysis. All data were log transformed prior to analysis, then means were back transformed for this table (see text for details). When ratios were significantly affected ($p < 0.05$), they are shown in bold, with the degree of confidence denoted with asterisks (* < 0.05 , ** < 0.01 , *** < 0.001).

	Volume (slope)	Fe-1/Ctrl Fe-2/Ctrl	Diatom/flagellate	Chl <i>a</i> (no/yes)
North				
S:C	0.109***	1.22* 0.78**	—	0.99
P:C	0.061*	1.34** 0.97	—	1.33***
P:S	-0.039	1.14 1.26*	—	1.36***
South				
S:C	0.063*	0.86 1.41**	0.70**	1.04
P:C	0.038	0.77* 1.71***	0.61***	1.45**
P:S	0.001	0.86 1.33*	0.96	1.46**

Results

Approximately 10–20 cells of each type from each of the eight stations were analyzed (268 cells in total). Diatoms were initially rare at the North Patch stations, and very few were observed on the EM grids. Thus, all diatom data are for cells from the South Patch. The volume-normalized element concentrations for all cells spanned four orders of magnitude (Fig. 1). Mean volume-normalized metal concentrations for the three cell groups are presented in Table 2.

Cellular P and S were highly correlated with estimated cellular C in both patches. Linear regressions of P versus C and S versus C in North Patch cells explained 93% and 95% of the variance, respectively. These relationships were only

Table 4. ANCOVA analysis of Mn:C, Mn:S, Ni:C, Ni:S, Zn:C, and Zn:S in the North and South patches. All data were log transformed prior to analysis, then means were back transformed for this table (refer to text for details). Significant differences in ratios ($p < 0.05$) are shown in bold, with the degree of confidence denoted with asterisks (* < 0.05 , ** < 0.01 , *** < 0.001).

	Volume (slope)	Fe-1/crtl Fe-2/crtl	Diatom/flagellate	Chl <i>a</i> (no/yes)
North				
Mn:C	-0.203**	1.53* 2.62***	—	1.07
Mn:S	-0.343***	1.51* 3.62***	—	1.19
Ni:C	-0.363***	1.50 2.17**	—	1.31
Ni:S	-0.456***	1.48 3.24***	—	1.35
Zn:C	0.122**	1.00 1.52**	—	1.28
Zn:S	0.079	1.17 2.13**	—	1.76**
South				
Mn:C	0.109	0.79 1.78**	0.90	1.11
Mn:S	0.025	0.84 1.42	1.79**	1.37
Ni:C	-0.060	0.80 1.24	1.84**	1.35
Ni:S	-0.118*	0.70 0.68	2.98***	1.24
Zn:C	0.215***	0.75 2.49***	1.49	2.36***
Zn:S	0.126*	0.79 1.77*	2.64***	2.12**

slightly weaker in the South Patch, where the presence of both diatoms and flagellated cells introduced some scatter, lowering the r^2 to 0.76 and 0.87 for P versus C and S versus C, respectively. The arithmetic mean molar ratio of C:P for all cells was 72.

Table 5. Least-squares mean station ratios and relative effects of cell volume and Fe addition on cellular Si:C, Si:S, Si:P, S:C, and P:C in diatoms from the South patch as determined by ANCOVA analysis. All data were log transformed prior to analysis, then means were back transformed for this table (refer to text for details). Significant differences in ratios ($p < 0.05$) are shown in bold, with the degree of confidence denoted with asterisks (* < 0.05 , ** < 0.01 , *** < 0.001). The final four columns display the least-squares mean ratios for diatoms at the four South patch stations.

	Volume (slope)	Fe-1/crtl Fe-2/crtl	High Fe/low Fe	Sta. 19 Pre	Sta. 24 Fe-1	Sta. 26 Fe-2	Sta. 27 Out
Si:C	0.406***	0.63** 1.10	0.83	0.50	0.31	0.47	0.36
Si:S	0.243***	0.48** 0.58*	0.52**	95	41	43	59
Si:P	0.144*	0.61* 0.55*	0.58**	63	38	26	42
S:C†	0.150**	1.14 1.60**	1.34*	5.8	7.2	10.7	8.1
P:C†	0.254***	1.03 1.95**	1.39	7.8	8.0	17.3	8.6

† mmol mol⁻¹.

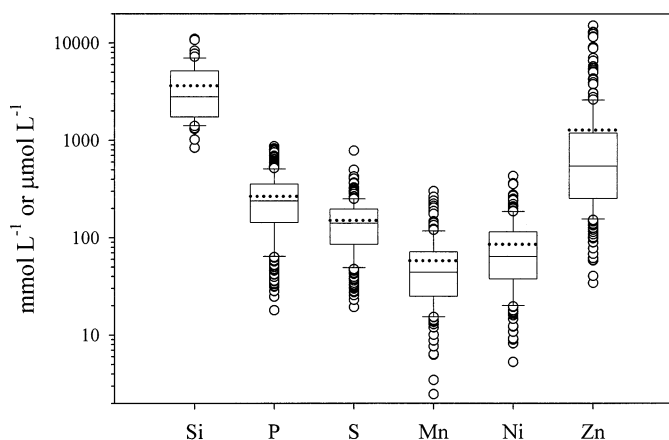


Fig. 1. Box plots of P, S, Mn, Ni, and Zn concentrations for all cells analyzed with SXRF; Si concentration is shown for diatoms only. The Si, P, and S concentrations are given as mmol L^{-1} , and the Mn, Ni, and Zn concentrations are given as $\mu\text{mol L}^{-1}$. In these plots, the solid line represents the median, the dotted line represents the arithmetic mean, the box delineates the 25th and 75th percentile confidence intervals, and the error bars encompass the 10th and 90th percentile confidence intervals. Data falling outside of these ranges are plotted individually.

Cellular S and P responded to Fe addition and varied with site, although patterns were complex (Tables 1, 3). After the first Fe addition to the North Patch, the least-squares mean P:C and S:C ratios increased 34% and 22% above ratios in unfertilized waters to 26 and 15 mmol mol^{-1} , respectively. Following the second Fe addition, the P:C ratio returned to the initial level while the S:C ratios dropped 22% below the ratios at the control (Pre and Out) stations. Similar changes were observed in the South Patch, but the timing was reversed. There, P:C and S:C dropped 23% and 14% after the first fertilization, but both ratios doubled following the second fertilization, resulting in ratios 71% and 41% higher than at the control stations. With the exception of the initial drop in South Patch S:C ratios, all of these changes were statistically significant ($p < 0.05$). Phosphorus increased significantly relative to S in both patches after the second input of Fe. Both P and S were approximately 30% lower, relative to C, in the unfertilized waters of the South Patch than in unfertilized North Patch waters.

Larger cells displayed higher P:C and S:C ratios in both patches, although the relationship between cell volume and P:C ratio in the South patch was not significant ($p = 0.23$; Table 3). Phosphorus:sulfur ratios were not significantly correlated with cell volume in either patch. Heterotrophic cells (those cells lacking Chl *a*) in both patches contained 33–46% ($p < 0.01$) more P than autotrophs relative to both C and S, while S:C ratios were essentially identical in heterotrophs and autotrophs from both patches. Grouped together, flagellated cells had 30–39% ($p < 0.01$) higher P:C and S:C ratios than diatoms in the South patch, but P:S ratios were not significantly different in the two groups.

Mean Mn:C, Ni:C, and Zn:C ratios tended to increase after Fe fertilization and were related to cell volume (Tables 1, 4). In the North Patch, Mn and Ni quotas rose approximately 50% after the first fertilization while Zn quotas

stayed constant. Following the second Fe addition, Mn:C, Ni:C, and Zn:C ratios rose 52–162% ($p < 0.05$) above ratios in the unfertilized cells. Metal quotas of South Patch cells remained unchanged following the first fertilization. After the second addition, however, Mn:C and Ni:C ratios increased 78% ($p < 0.01$) and 24% ($p < 0.05$) relative to the control stations, and the mean Zn:C ratio of resident cells more than doubled ($p < 0.001$). Cell volume was negatively correlated to Mn and Ni but positively correlated to Zn in North Patch cells ($p < 0.01$). Significant volume relationships were not observed in the South Patch for Mn and Ni, but Zn:C ratios were again higher in larger cells ($p < 0.001$). Manganese and Ni quotas were not significantly different in heterotrophs and autotrophs, but Zn:C ratios were 136% higher in South Patch heterotrophs. Diatoms displayed notably higher (84%; $p < 0.01$) Ni:C ratios than flagellated cells.

In general, cellular Si normalized to C, S, and P decreased following Fe fertilization and was positively related to cell volume (Table 5). All three Si quotas were lower at the Out station than the Pre station, weakening the observed changes resulting from the Fe addition, but Si:C, Si:S, and Si:P dropped 37–52% ($p < 0.05$) following the first fertilization. Silicon:carbon returned to the pre-fertilization levels after the second Fe injection. With the two in-patch stations grouped to increase statistical power, Si:S and Si:P were 42–48% ($p < 0.01$) lower in fertilized cells than in unfertilized cells. Cellular Si was positively correlated to diatom cell volume ($p < 0.05$) whether normalized to C, S, or P.

Several consistent trends in the distribution of elements were noted among the cells. With the exception of Si in diatoms, which mapped onto the frustules, elements were typically localized centrally within the cells and not distributed evenly over the surface (Fig. 2). Phosphorus and zinc were frequently colocalized in diverse cells, suggesting that these elements are concentrated in the same cell structures. In autotrophic cells, Fe was often most highly concentrated in the region of the chloroplast, identified by its red auto-fluorescence under blue light. Manganese and nickel concentrations were generally characterized by less structure, although several centric diatoms scanned in valve view exhibited a ring of Ni concentrated around the circumference of the cell (see also Twining et al. 2003).

Discussion

This study contributes some of the first unequivocal data on the trace-metal composition of nanoplankton cells collected from natural waters. Only a few studies have reliably measured the trace-metal concentrations in natural plankton assemblages, and all of these have relied on either filtration to concentrate cells for bulk analysis (e.g., Martin and Knauer 1973; Collier and Edmond 1984; Cullen et al. 2003) or have involved macroscopic aggregates such as *Trichodesmium* tufts that can be isolated manually from the water for analysis (e.g., Berman-Frank et al. 2001). In contrast, the SXRF technique allows us to specifically target individual cells for analysis. This ensures that our analyses are not biased by abiotic material (not attached to the target cells but

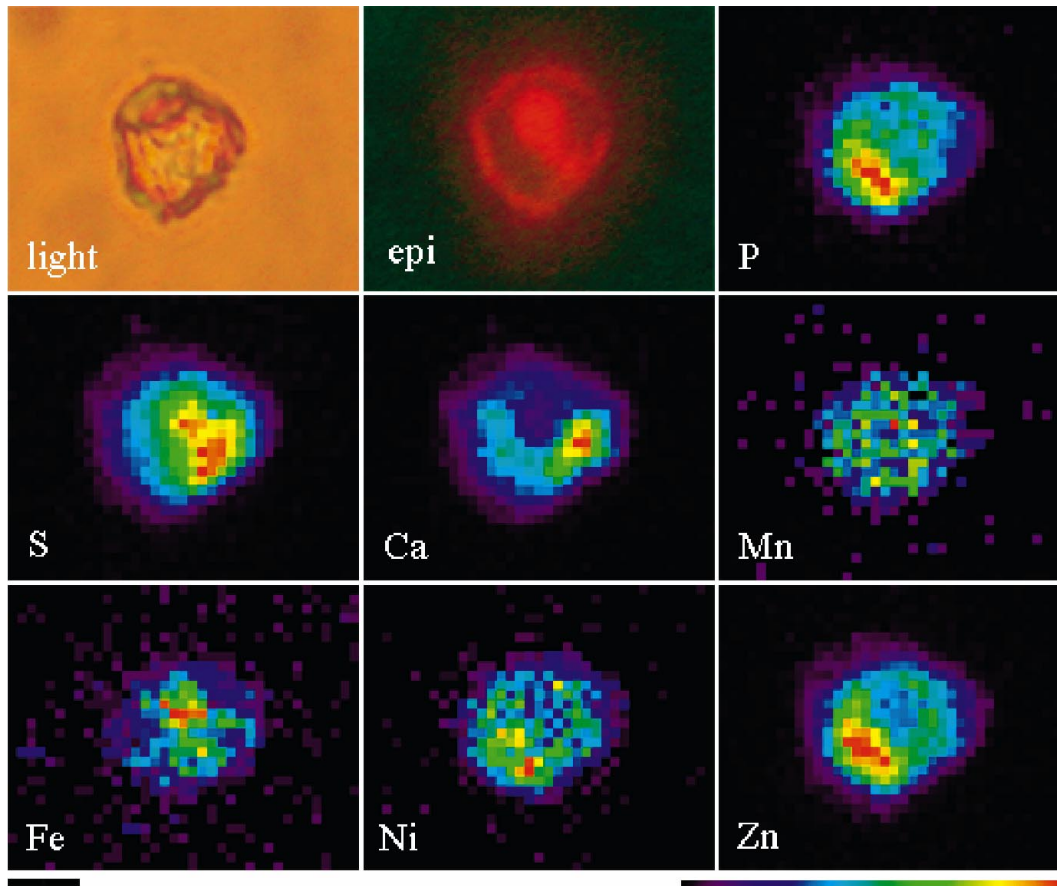


Fig. 2. Light and epifluorescence micrographs and SXRF false-color element maps of an autotrophic flagellated cell from the Southern Ocean. Each SXRF image provides the relative distribution of the specific element, and thus, the absolute concentration scales vary for each image (SXRF map scale bar = 5 μm). The red autofluorescence indicates the presence of Chl *a*.

caught on filters), and it also allows us to compare the element stoichiometries of functionally diverse, but similarly sized, plankton.

When considering trace-element stoichiometries in cells, several different elements may be used as a proxy for cellular biomass; each may be appropriate under different circumstances. When studying the link between trace metals and C cycling, it is logical to normalize metal contents directly to cellular C. When investigating the interplay of trace metals and macronutrients, it may be more useful to normalize metals directly to cellular N or P. In some cases, technical limitations will constrain the choice of a biomass proxy. For example, bulk particulate-metal samples are typically collected on acid-leached polycarbonate membranes, which mask the C signal of the trapped particles. In these situations, geochemists may normalize to P, which can be measured directly with inductively coupled plasma mass spectrometry (ICP-MS). Cellular C is then calculated from either C:P ratios measured separately or from the Redfield ratio. The phosphorus content of plankton, however, can be highly elastic, varying with ambient light, growth rate, and available P (Sterner and Elser 2002). Thus, P may not be the best proxy for overall cell biomass.

Sulfur may serve as a more consistent proxy of cellular biomass. Like N, sulfur is an important component of many

organic molecules related to cell structure, particularly proteins. Unlike N and P, however, S is abundant and homogeneously distributed in the ocean, and S:C ratios in aquatic protists appear to be relatively stable. Further, there is good agreement between published measurements of S:C in a variety of aquatic organisms (Cuhel and Waterbury 1984; Cook and Kelly 1992; Payne and Price 1999), and C and S were highly correlated in the cells analyzed with SXRF. Given that S was measured simultaneously with the trace metals in each cell, we repeated the ANCOVA analyses with S-normalized element quotas to confirm the trends noted for the C-normalized stoichiometries (Tables 3–5).

The observation that P:C and S:C ratios—but not P:S ratios—were positively related to cell volume raises the possibility that C was underestimated by our methods. Unlike the rest of the elements, cellular C was not measured directly with SXRF but was calculated from cell BV, which was calculated from linear cell dimensions. Most published C:BV relationships, including those of Menden-Deuer and Lessard (2000) used in this study, are calculated for hydrated cells. If the target cells analyzed here experienced significant cell shrinkage upon drying, then our approach would tend to underestimate the C content of these cells. Cells lacking rigid cell walls or frustules, such as flagellates and naked dinoflagellates, would be expected to shrink more than cells

possessing these structures, such as diatoms. Thus, shrinkage might explain the approximately 20% higher S:C and P:C ratios observed for flagellated cells, as compared with diatoms. Additionally, the C:volume equations of Menden-Deuer and Lessard (2000) are not linear; rather, the C:BV conversion factors are power functions that decrease as cell BV increases. This relationship, appropriate for hydrated cells, may not apply to dried cells.

The choice of a C:BV conversion factor will also impact the C stoichiometries. Numerous studies have investigated the C:BV relationship in various plankton groups (e.g., Strathmann 1967; Moal et al. 1987; Montagnes et al. 1994), and each has reported a different relationship. We chose the equations of Menden-Deuer and Lessard (2000) because their C:BV relationships were developed with data combined from many of these studies. However, calculated cellular C would be only marginally different if the other equations were used. Carbon cell⁻¹ was found to be 12% and 23% lower, on average, using the equations of Strathmann (1967) and Montagnes et al. (1994) but 23% higher using the equation of Moal et al. (1987). Therefore, the cellular-C values calculated with the Menden-Deuer and Lessard equation represent a central estimate.

Cell shrinkage may also have resulted from chemical fixation with 0.25% glutaraldehyde. Verity et al. (1992) observed BV to decrease an average of 29% following fixation with 0.5% glutaraldehyde, and Booth (1987) reported a similar effect with 2.5% glutaraldehyde. However, Menden-Deuer et al. (2001) found highly variable changes in diatom and dinoflagellate BVs after fixation with 1% glutaraldehyde, with some taxa shrinking up to 50% and some swelling nearly 30%. On average, thecate dinoflagellate BVs increased 16%, athecate dinoflagellate BVs decreased 9%, and diatom BVs were 7% lower. However, because there was a great deal of variability among individual species, biomass estimates for mixed assemblages of fixed cells were not significantly different from estimates for live cells (Menden-Deuer et al. 2001). As the diatom, autotrophic flagellate, and heterotrophic flagellate groups in this study were each comprised of numerous different species, it is therefore likely that the overall mean C content of each group would not have been significantly different for unfixed cells.

While it is possible that shrinkage during drying or fixation caused an underestimation of cellular C, the S:C ratios measured for the individual cells were at the lower end of the range of values measured for cultured phytoplankton by Payne and Price (1999). These researchers recorded S:C ratios of 7.6–23 mmol mol⁻¹ for cultured dinoflagellates, diatoms, and prymnesiophytes, while we found mean diatom and flagellate ratios of 7.8 and 11.4. Although Payne and Price (1999) did not observe systematic differences in the S:C ratios of diatoms and flagellated cells, their mean S:C ratio for all eight phytoplankton species examined was 15.3 mmol mol⁻¹, 50% higher than the overall geometric mean S:C ratio of 10.5 mmol mol⁻¹ measured for all SOFeX cells. A mean S:C ratio of 15.9 mmol mol⁻¹ was calculated from data collected for 14 marine phytoplankters by Ho et al. (2003), with diatoms containing threefold higher S:C than flagellates (Table 6). If C was underestimated, the S:C ratios would be expected to fall above, not below, the published

culture data. Reported S:C ratios similar to the SOFeX values reported here exist for marine *Synechococcus* (10.5 mmol mol⁻¹; Cuhel and Waterbury 1984) and freshwater algae (10 mmol mol⁻¹; Cook and Kelly 1992). Therefore, it is very unlikely that C was underestimated in the cells of this study.

Different stoichiometries of cell groups—Regardless of whether cellular elements are normalized to calculated cell C or measured cell S, significant differences were observed in the elemental composition of diatoms and autotrophic and heterotrophic flagellates. The higher P content of heterotrophs observed in both patches, despite their different plankton assemblages, likely represent real physiological differences. In many organisms, most of the P is incorporated in nucleic acids within the ribosomes (Sterner and Elser 2002). Cellular RNA is closely related to growth rate in phytoplankton and zooplankton (Sutcliffe 1965; Dortch et al. 1983), and the fast growth rates characteristic of heterotrophic protozoa may require more P, relative to autotrophs. Stoecker and Capuzzo (1990) report that protozoa generally have higher N:C ratios than phytoplankton, as well. Additionally, autotrophs must invest a considerable amount of cellular material into photosynthetic machinery. Because photosynthetic pigments and proteins, as well as cell walls, all contain C but little P, it follows that autotrophs might be expected to have lower P:C ratios than heterotrophs.

The 40% higher P content of heterotrophs is matched by ~100% higher Zn quotas in both patches (Fig. 3), and Zn and P were frequently collocated in the cells. This association is not surprising given the important roles Zn finger proteins play in the repair and transcription of nucleic acids. Zinc is incorporated in the enzymes RNA/DNA polymerase, reverse transcriptase, and tRNA synthetase, among others. Thus, it appears that the higher RNA and P content of the heterotrophic cells may result in correspondingly higher Zn stoichiometries as well. In contrast, Mn and Ni quotas were not significantly different among autotrophic and heterotrophic cells. Zinc is also incorporated in the enzyme carbonic anhydrase (CA), which catalyzes the hydration/dehydration of CO₂. Both heterotrophs and autotrophs contain mitochondrial CA, but phytoplankton might be expected to include additional CA associated with photosynthetic C fixation. However, CA would account for a smaller portion of the cellular Zn in phytoplankton if Cd or Co substitute for Zn in CA, as has been observed for some phytoplankton species grown at low Zn concentrations (Price and Morel 1990).

While P quotas did not vary between diatoms and flagellates relative to S, metal ratios were all higher in diatoms than in flagellated cells (Fig. 3). Manganese is a constituent of the O₂-evolving enzyme in Photosystem II, as well as many other proteins, including superoxide dismutase. The principal use of Ni in eukaryotes is in urease, the enzyme that hydrolyzes urea to ammonia for subsequent use by the cell. In several of the centric diatoms, the Ni mapped onto the outer edge of the cell, suggesting that this element was present mostly along the girdle of the frustule. Laboratory studies have found that a range of diatoms and flagellated cells use urease to access urea for a source of N (Oliveira and Antia 1986), but it has not been shown that diatoms

Table 6. Elemental composition (ratios normalized to cellular P and C) of cultured phytoplankton and natural plankton assemblages as measured with bulk analysis and SXRF (this study). Shown are geometric mean (n) stoichiometries for each cell type (diatoms, autotrophic flagellated cells—A flag, heterotrophic flagellated cells—H flag) collected from either low Fe (Pre and Out) or high Fe (Fe-1 and Fe-2) stations. The SXRF Fe data is from Twining et al. (2004).

	Monterey Bay ^a		N. Pacific Ocean ^b		Southern Ocean ^c		Algal cultures ^d			This study (low Fe)			This study (high Fe)		
							Diatom	A flag	Diatom	A flag	H flag	Diatom	A flag	H flag	
Elements normalized to P															
C	—	—	—	66	62	147	112 (19)	61 (26)	112 (19)	61 (26)	45 (40)	96 (37)	53 (60)	42 (68)	
S	—	—	—	—	1.8	1.1	0.74 (18)	0.69 (26)	0.74 (18)	0.69 (26)	0.54 (40)	0.79 (37)	0.63 (61)	0.47 (67)	
Mn [†]	0.39	0.34	1.68	—	2.9	4.1	0.42 (14)	0.16 (16)	0.42 (14)	0.16 (16)	0.14 (32)	0.28 (24)	0.22 (36)	0.17 (35)	
Fe [†]	5.2	4.6	—	—	3.0	9.1	0.71 (14)	0.54 (23)	0.71 (14)	0.54 (23)	0.63 (39)	1.93 (34)	1.93 (60)	0.94 (66)	
Ni [†]	0.21	0.86	—	—	—	—	1.15 (18)	0.16 (18)	1.15 (18)	0.22 (29)	0.22 (29)	0.73 (34)	0.21 (21)	0.20 (44)	
Zn [†]	0.84	3.0	11.09	—	0.52	0.90	8.1 (18)	1.4 (26)	8.1 (18)	1.4 (26)	2.1 (39)	6.2 (36)	1.8 (59)	2.6 (60)	
Elements normalized to C															
P [†]	—	—	—	15.2	17.7	8.1	9.0 (19)	16.4 (26)	9.0 (19)	16.4 (26)	22.0 (40)	10.4 (37)	18.7 (60)	23.7 (68)	
S [†]	—	—	—	—	32.9	9.1	6.8 (18)	11.3 (26)	6.8 (18)	11.3 (26)	11.9 (41)	8.3 (38)	11.7 (61)	11.0 (69)	
Mn [†]	—	—	—	25.5	46.7	36.7	3.4 (13)	2.7 (14)	3.4 (13)	2.7 (14)	3.0 (33)	4.5 (25)	4.4 (35)	4.4 (34)	
Fe [†]	—	—	—	—	47.4	61.9	6.0 (15)	8.7 (25)	6.0 (15)	8.7 (25)	14.1 (40)	22.8 (38)	36.1 (60)	21.9 (69)	
Ni [†]	—	—	—	—	—	—	7.8 (15)	2.7 (17)	7.8 (15)	2.7 (17)	4.9 (29)	8.5 (36)	4.3 (21)	5.4 (44)	
Zn [†]	—	—	—	168	7.5	6.0	67.8 (18)	22.2 (27)	67.8 (18)	22.2 (27)	46.9 (40)	70.7 (38)	34.0 (60)	60.0 (62)	

^a Martin and Knauer (1973); data shown are selected by Bruland et al. (1991). Cells were collected with a 76- μ m net during a diatom bloom.

^b Collier and Edmond (1984); data shown as selected by Bruland et al. (1991). Mixed assemblages of plankton cells were collected with a 44- μ m net.

^c Cullen et al. (2003); cells were collected on 0.45- μ m membranes. Community biomass was dominated by diatoms.

^d Ho et al. (2003); data shown are means of flagellated cells ($n = 11$) and diatoms ($n = 4$) grown in metal-replete media.

[†] mmol mol⁻¹.

[‡] μ mol mol⁻¹.

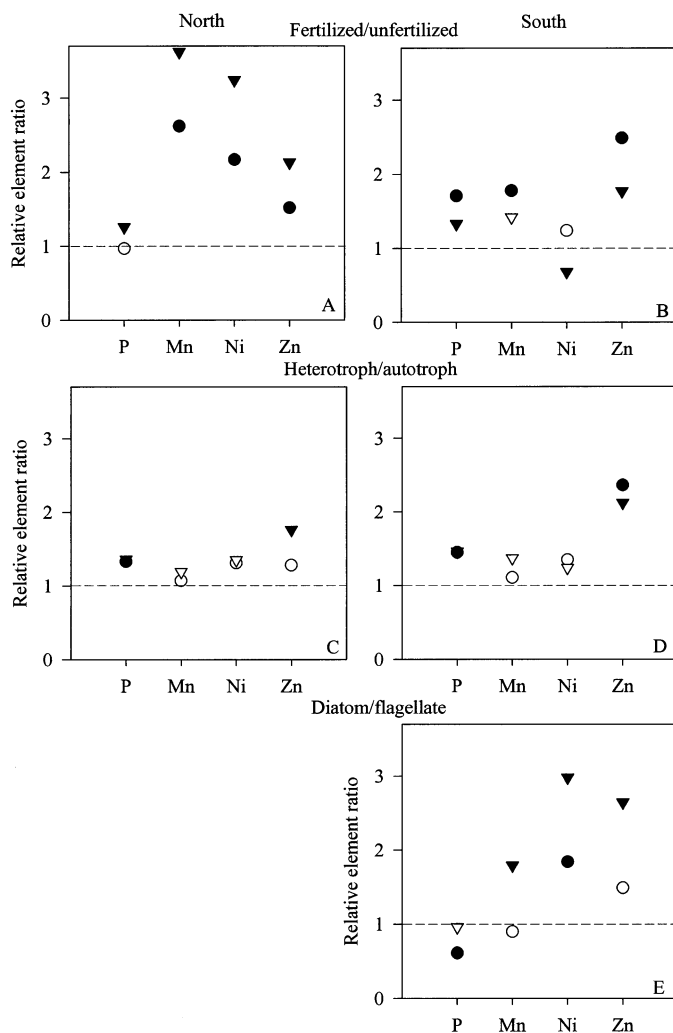


Fig. 3. Influence of Fe fertilization and cell type (heterotroph vs. autotroph or diatom vs. flagellate) on cellular P, Mn, Ni, and Zn quotas in the North and South Patches. In panels A and B, the ANCOVA effect ratios of In-Patch element quotas to Out-Patch element quotas are plotted. Panels (C) and (D) show the ANCOVA effect ratios of heterotroph element quotas to autotroph element quotas. Panel (E) displays the ANCOVA effect ratios of diatom element quotas to flagellate element quotas in the South Patch. Data are shown for element quotas normalized to both cellular C calculated from cell volume (circles) and cellular S measured directly with SXRF (triangles). For Fe fertilization, element quotas in cells collected after the second Fe addition are compared with quotas in cells collected from outside the fertilized patch (Pre and Out station cells combined). Ratios found to be statistically significant (i.e., the ratio is significantly different than 1, $p < 0.05$; see text for details) are indicated by black symbols, while ratios with $p > 0.05$ are shown in white.

have a greater affinity for this mode of N acquisition than flagellated cells. Hence, it is not clear why diatoms display a greater concentration of Ni than flagellated cells. As mentioned above, Zn is required for both nucleic acid transcription and repair proteins, as well as for alkaline phosphatase and carbonic anhydrase. The causes of these differences are not immediately apparent, and future studies should deter-

mine if these trends are present in other areas and at other times.

Significant relationships were detected between the trace-metal stoichiometries and cell volume. In general, Mn and Ni quotas were negatively correlated with cell volume in both patches, as was observed for cellular Fe (Twining et al. in press). This relationship was not an artifact of C estimation errors because the trend is stronger in the S-normalized Mn and Ni quotas (Table 4). Because smaller cells have larger surface area: volume ratios, they should be characterized by higher concentrations of surface-reactive metals. Cellular Zn shows the opposite relationship, with larger cells having higher Zn:C and Zn:S ratios. It is not clear why this metal would have a different relationship to cell volume, but we note that the concentration of cellular P, which was frequently colocated with Zn, was also positively correlated with cell volume.

The SXRF element maps indicate that metals were concentrated within the biomass and were not merely sorbed to the outer surfaces of the cells. Surface-bound elements would either be evenly distributed in relatively flat cells or more concentrated at the edges in thicker cells where the X-ray beam irradiates more of the cell surface area. Silicon showed the latter distribution in the diatom maps. Alternatively, metals concentrated evenly throughout the biomass would appear higher in the center of the cell, where the cell is presumed to be thicker, and metals concentrated in organelles would map onto these structures. Normally, Mn, Ni, and Zn all showed a central localization within cells, indicating that these metals were not predominantly externally sorbed. A similar result was observed for Fe in the cells collected both before and after fertilization (Twining et al. in press). These distributions do not indicate that all of the metal was located internally, but only that most of the metal associated with the cells was internal. It is unlikely that the Ni rings observed around several of the centric diatoms scanned in valve view resulted from surface adsorption or coprecipitation alone because Si exhibited a much more even distribution. Concentration of Ni along the girdle of the diatom would produce the observed distribution, but there are too few examples of this pattern to establish its generality.

Changing stoichiometries following fertilization—In addition to the varying metal stoichiometries observed for the different cell groups, the trace-element contents of resident cells changed markedly as they responded to the added Fe. In the North, P:C increased within the patch after the first fertilization, while in the South, plankton P:C did not increase until after the second addition. The timing of these stoichiometric shifts mirror the changes in Chl *a* in both patches. In the North, total Chl *a* at 20 m nearly doubled after the first Fe addition (from 0.140 mg m^{-3} at the Pre station to 0.254 mg m^{-3} at the Fe-1 station; V. Lance pers. comm.), but actually decreased slightly after the second addition (0.224 mg m^{-3}). Similarly, P:C increased by 34% after the first Fe addition but then returned to the level of the reference station following the second fertilization. Cell growth (as indicated by changes in Chl *a*) and plankton P:C were also synchronized in the South; there, the phytoplankton responded more slowly to the Fe enrichment, per-

haps because of the markedly colder water temperatures (-0.54°C at 20 m compared with 6.5°C at 20 m in the North patch). Chlorophyll increased only 50% between the Pre and Fe-1 stations (from 0.258 to 0.393 mg m^{-3}), while P:C actually decreased 23%. Between the Fe-1 and Fe-2 stations, however, Chl *a* rose another 79% (to 0.704 mg m^{-3}) and was matched by increased P:C, which was 71% higher than at reference stations. Thus, community growth response and P:C ratios appear to be related. These results support the growth rate hypothesis of Sterner and Elser (2002), which suggests that organismal variations in ribosomal RNA needed for rapid growth are reflected in the P:C stoichiometries of the organisms, resulting in higher P:C ratios in rapidly growing organisms.

Cellular trace-metal quotas generally remained constant or increased slightly following the first fertilization and then rose further following the second fertilization. This trend was seen in both patches, although the magnitude of observed effects differed somewhat (Fig. 3). It is not immediately clear why all three metals would be accumulated following fertilization. As noted above, Mn, Ni, and Zn are components of cellular proteins involved in energy-yielding processes, nutrient acquisition, and the production of cellular material. Consequently, each may have been required in increasing quantities as constraints on primary production and cell growth were removed by fertilization (Coale et al. 2004). This raises the possibility that the Sterner and Elser (2002) growth rate hypothesis used to explain variability in C:P ratios can be extended to Mn:C, Ni:C, and Zn:C. Indeed, Mn:P, Ni:P, and Zn:P ratios don't systematically increase after Fe addition (Table 6; $p = 0.97$, $n = 9$; two-tailed pairwise *t*-test), suggesting that, on average, these metals increase in proportion to P as cell growth increases. In reality, the response of the P normalized metal ratios to Fe addition is fairly uniform across the metals but unique to each cell type. Based on Table 6, diatom metal:P ratios decrease by 31% (SD = 7%), while autotrophic flagellate metal:P ratios increase 32% (SD = 5%) and Mn:P and Zn:P increase 23% in heterotrophic flagellates. The distinct responses to Fe addition may reflect interspecific differences in the allocations of cellular resources to P-rich and metal-rich cellular components during fast growth.

Unlike Mn and Zn, which are involved in a variety of cellular functions, Ni is almost exclusively used as a cofactor in urease (Oliveira and Antia 1986). Given the high NO_3^- concentrations present in both patches ($22\text{--}30\ \mu\text{mol L}^{-1}$), it is unclear how important dissolved organic nitrogen was as a source of N for resident plankton. Still, phytoplankton have been found to produce urease regardless of the N source being utilized (Fan et al. 2003), and urease activity appears to increase with growth rate. Further, Peers et al. (2000) observed nutrient-replete diatom cultures to increase urease activity when grown on nitrate. Gordon et al. (1998) did not note significant increases in particulate Mn, Ni, or Zn following fertilization during IronEx-I, but Ni concentrations in the $>5\text{-}\mu\text{m}$ fraction did increase immediately following the addition of Fe to the patch.

The Si stoichiometries of diatoms in the South Patch also changed following fertilization. Bulk measurements of Si in both field-collected and laboratory-cultured populations of

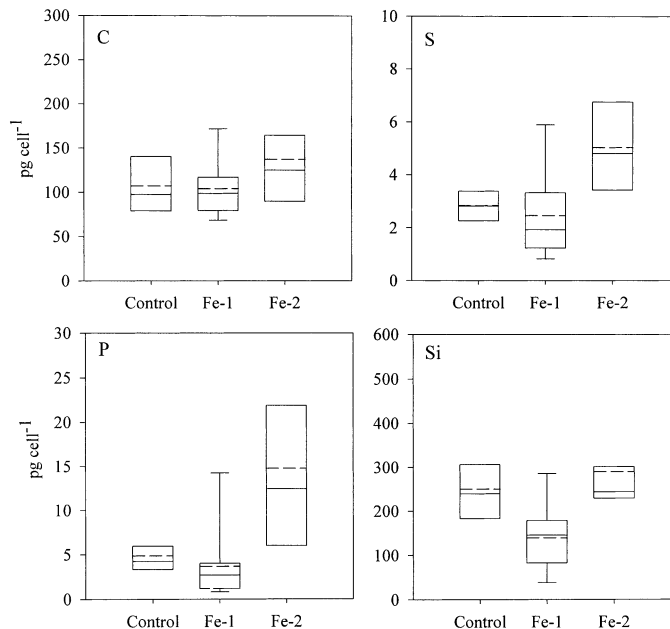


Fig. 4. Box plots of cellular C, S, P, and Si contents for *Fragilariopsis* sp. diatoms collected from the South Patch. Each elemental concentration is shown for the Control stations (Pre and Out stations combined), as well as for the stations sampled immediately following the first (Fe-1) and second (Fe-2) Fe additions. In these plots, the solid line represents the median, the dotted line is the arithmetic mean, the box delineates the 25th and 75th percentile confidence intervals, and the error bars encompass the 10th and 90th percentile confidence intervals.

diatoms have shown that these cells become more highly silicified when their growth is limited by availability of other nutrients (Hutchins and Bruland 1998; De La Rocha et al. 2000). We found Si:S and Si:P to be significantly lower inside the patch. While these results appear to be generally consistent with the findings of Hutchins and Bruland (1998), the lower Si stoichiometries at the two in-patch stations result from different effects. After the first addition, Si:C, Si:P, and Si:S dropped 37–52% while C cell⁻¹, P cell⁻¹, and S cell⁻¹ remained unchanged. Following the second fertilization, however, the mean Si:C ratio for diatoms in the patch returned to the level seen at the control stations. Meanwhile, Si:S and Si:P ratios remained lower as a result of increasing diatom P:C and S:C ratios at this time (Table 5). Therefore, the lower Si:P and Si:S ratios were initially caused by decreasing Si per cell but later caused by higher P and S per cell. Because the C content of the diatoms was estimated from cell volume (which did not change markedly during the experiment), a similar change was not seen in the Si:C ratio.

These trends are shown even more clearly in the data for *Fragilariopsis* sp. diatoms, which were easily identified on the grids. As shown in Fig. 4, C cell⁻¹ did not change markedly following fertilization. Cellular Si fell 44% following the first Fe addition and then actually rose 16% above that observed in the control (unfertilized) stations. Cellular S and P fell slightly at the Fe-1 station and then increased 179% and 305%, respectively, at the Fe-2 station. The resulting

Fragilariopsis Si:S and Si:P stoichiometries were 32% and 42% lower after two Fe additions. These changes are similar to those observed in bottle incubations and laboratory cultures by Takeda (1998). He found that $\text{Si(OH)}_4:\text{PO}_4^{3-}$ utilization ratios decreased in incubations of Southern Ocean and subarctic North Pacific waters amended with Fe, as compared with control bottles receiving no Fe. In subsequent laboratory incubations of two diatom species isolated from the Southern Ocean, Takeda (1998) found that the shift in cellular Si:P was caused by a change in cellular Si in one species and by a change in cellular P for the other. Our data indicate that the observed change in Si:P (and Si:S) ratios resulted from a combination of these two effects. Matching changes were not seen for Si:C ratios because cellular C was estimated from cell volume, which, because it is constrained by the size of the diatom frustules, remained constant following fertilization.

Comparison with other studies—Mean elemental ratios of diatoms, autotrophic flagellates, and heterotrophic flagellates collected from low-Fe (Pre and Out stations) and high-Fe (Fe-1 and Fe-2) waters during SOFeX are compared with published bulk studies of plankton composition in Table 6. Also shown are data from a laboratory study of metal stoichiometries in cultured phytoplankton. The mean diatom C:P ratio of 104 measured with SXRF is nearly identical to the Redfield ratio of 106. The C:P ratios of flagellates were approximately 50% lower, closer to the C:P ratio of 66 measured for bulk Southern Ocean plankton by Cullen et al. (2003). This similarity is curious because the authors report their plankton assemblages to be dominated by diatom species (although *Phaeocystis* was also present). Others have also noted the relative enrichment of P in phytoplankton, and diatoms in particular, in the Southern Ocean (De Baar et al. 1997). In contrast with the SXRF data for field-collected phytoplankton, Ho et al. (2003) found the mean C:P ratio of diatoms (62, $n = 4$) to be less than half the mean ratio of flagellates (147, $n = 11$) in laboratory cultures. Although a 106:1 C:P ratio is frequently invoked as representative of all marine plankton, C:P ratios can vary widely between species of plankton and nutrient regimes. While Ho et al. (2003) present a mean C:P ratio of 124 (data for HCl-fumed filters), they observed C:P to range from 42 to 222 for cultured algae, and Geider and La Roche (2002) found a wide range of C:P reported for both bulk marine particulate matter (35–221) and cultured phytoplankton (27–135) in the literature. In fact, they report an average C:P ratio for phytoplankton grown in nutrient-replete cultures of 75. Furthermore, these authors note that P appears to be relatively enriched (relative to N, but presumably also to cellular C) in plankton material from N- and P-rich waters (e.g., Menzel and Ryther 1964).

Earlier single-cell studies of plankton stoichiometries have shown C:P stoichiometries to vary widely in cells collected from the same waters. An electron microprobe (XRMA) study of heterotrophic bacterioplankton from the Sargasso Sea reported C:P to range from 59–143, but noted that previous XRMA studies of bacteria in coastal, brackish, and freshwater systems had found much lower C:P ratios (~13–

33) (Gundersen et al. 2002). Cellular C and P were quantified in individual cells of the dinoflagellate *Dinophysis norvegica* with a proton microprobe by Gisselson et al. (2001). The mean C:P ratio of 30 cells was 383 ± 114 , but this number was skewed by the high C:P ratios of the dinoflagellates' thecae, which were three times higher than overall cellular C:P ratios (mean ~1,500). Therefore, it is difficult to compare their results with ours.

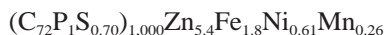
Given the close agreement between the diatom C:P ratios and Redfield and the possibility that C was underestimated in flagellates, we also calculated the mean C:P ratio of each group from the cellular S content using a S:C ratio of 10 mmol mol^{-1} (Cuhel and Waterbury 1984; Cook and Kelly 1992). This resulted in mean diatom, autotrophic flagellate, and heterotrophic flagellate C:P ratios of 67, 64, and 46, respectively, comparable with the C:P ratio of 66 measured by Cullen et al. (2003). These results are in contrast with those of Ho et al. (2003), who found cultured flagellates to have higher C:P ratios than diatoms. The lack of direct measurements of C in the cells analyzed here prevents us from conclusively determining the C:P ratio, but both methods of calculation indicate that flagellated cells are enriched in P relative to Redfield.

The Mn, Ni, and Zn stoichiometries are generally close to the values measured with bulk techniques on other field samples but depart somewhat from the ratios in cultured cells. The Mn contents of both diatoms and flagellates were close to the bulk results of Martin and Knauer (1973) and Collier and Edmond (1984) but are almost an order of magnitude below those measured for Southern Ocean plankton (Cullen et al. 2003) or cultured cells (Ho et al. 2003). We have no ready explanation for the discrepancy with the Mn concentrations of Cullen et al. Ho et al. chose an unchelated Mn concentration (Mn') of 10 nmol L^{-1} for their culture media, approximately 10-fold higher than in the open ocean (Donat and Bruland 1995), and this may explain the higher Mn quotas of the cultured cells. While the diatom Ni:P ratios are close to the ratio measured in the North Pacific Ocean, our flagellate Ni:P ratios are nearly identical to those measured for bulk plankton in Monterey Bay. This similarity is unexpected because Martin and Knauer (1973) used a 76- μm plankton net to collect their sample, presumably retaining mostly large diatoms. We found diatoms to have higher Ni concentrations than flagellates. However, smaller cells also contained more Ni than larger cells. The similar Ni ratios in large diatoms and small flagellates may result from these offsetting effects. Single-cell Zn quotas fall between those measured by Martin and Knauer (1973) and Cullen et al. (2003), with diatom ratios approaching those measured by the latter study and flagellate ratios more closely approximating that measured by the former. The lower Zn:P ratios measured by Ho et al. (2003) may have resulted from biochemical substitution of Zn by Cd or Co, as suggested by these authors.

Comparisons of these metals in diatoms and flagellates are influenced by the choice of biomass proxy. While Martin and Knauer (1973) and Collier and Edmond (1984) reported only P-normalized metal ratios, Ho et al. (2003) measured both P and C in each species of phytoplankton. The latter researchers found Mn:P, Fe:P, and Zn:P ratios to be higher

in autotrophic flagellates than in diatoms, while, in each case, we observed the opposite trend. When normalized to cellular C, however, Mn and Zn appear higher in cultured diatoms than autotrophic flagellates. We observed similar differences between these two groups, although Mn and Zn are significantly ($p < 0.05$, Table 4) higher in diatoms only when normalized to cellular S. These discrepancies highlight the effects of choosing different proxies for cellular biomass. They also demonstrate the biases that may be introduced into interspecific or intergroup comparisons by converting between C and P using a single Redfield ratio.

Some researchers have suggested extending the Redfield ratio to include bioactive trace metals such as Mn, Fe, Ni, Co, Cu, Zn, and Cd (Morel and Hudson 1985). Bruland *et al.* (1991) developed such an extended Redfield ratio from three published studies of trace metals in bulk plankton, having noted the similarities in reported metal:P ratios. From their analyses of cultured phytoplankton, Ho *et al.* (2003) also calculated mean extended stoichiometries. The overall arithmetic mean element stoichiometry calculated for all cells analyzed in our study is



The stoichiometries in the overall extended Redfield ratio are each within a factor of three of those calculated by Bruland *et al.* (1991). The C and S ratios are each within a factor of two of the mean ratios for phytoplankton analyzed by Ho *et al.* (2003), while the Fe and Zn ratios are fourfold lower and sevenfold higher, respectively. These disparities are likely caused by differences in ambient metal chemistry, light regimes, and species composition.

While the general overall agreement between these extended stoichiometries suggests that the concept of the Redfield ratio can be applied to the bioactive trace metals, the data reported here show that some systematic variability between different types of protists exists in the metal stoichiometries of field-collected cells. This variability exceeds that found in the macronutrient ratios of the plankton. The ANCOVA revealed that the C and P contents of diatoms and flagellates (normalized to cellular S) differed by 30% or less, while the Mn, Ni, and Zn contents varied by 79–198%. Similarly, C and P changed by no more than 41% following two Fe additions, but Mn, Ni, and Zn ratios (again, normalized to S) typically increased by ~100–250%. Ho *et al.* (2003) also observed more variability in the metal:P ratios than the C:P ratios of different cell types. The relative standard error of C:P ratios (excluding $CaCO_3$ tests) for 15 species was 6%, but the relative standard error for the bioactive trace metals ranged from 16% to 28%. Given the higher variability of trace-metal content, the utility of an extended Redfield ratio will depend on the precision required for the specific application.

Redfield himself recognized that C:N:P ratios vary between cells (Redfield *et al.* 1963). Although various cellular components may be characterized by certain elemental stoichiometries, the proportion of these organelles likely varies between cell taxa and under different ambient conditions (Geider and La Roche 2002; Sterner and Elser 2002). Additionally, there is strong evidence for luxury uptake of N and P by phytoplankton (Rhee 1978), whereby cells will

store excess nutrients in vacuoles prior to use. Both autotrophic and heterotrophic protists have been shown to accumulate excess trace-metal nutrients as well (Sunda and Huntsman 1995; Chase and Price 1997), although antagonistic effects between trace metals are common (Sunda and Huntsman 1998). Therefore, it appears that plankton elemental composition is likely to vary both as a function of the ambient nutrient concentrations, cellular growth rates, and the taxonomic composition of the plankton assemblage. This is supported by the cell-specific data presented here.

To evaluate the degree of enrichment of metals in phytoplankton relative to ambient seawater, it is possible to calculate metal bioconcentration factors (on a volume basis) in all phytoplankton (diatoms and autotrophic flagellates) using the data presented in Table 2 and reported dissolved metal concentrations in Southern Ocean surface waters. Weighted mean volume-normalized concentration factors (VCFs), defined as mol metal μm^{-3} cell divided by mol metal dissolved μm^{-3} water, in the autotrophs are 4.0×10^5 for Mn (using a dissolved Mn concentration of 0.1 nmol L^{-1} ; Cullen *et al.* 2003), 3.6×10^6 for Fe (using a dissolved Fe concentration of 30 pmol L^{-1} ; Cullen *et al.* 2003), 1.6×10^4 for Ni (using a dissolved Ni concentration of 6 nmol L^{-1} ; Loscher 1999), and 6.7×10^5 for Zn (using a dissolved Zn concentration of 1 nmol L^{-1} ; Cullen *et al.* 2003). The Fe VCF is comparable with other reported values for phytoplankton, but the Mn, Ni, and Zn values are 7-fold, 5-fold, and 67-fold higher, respectively, than other reported values (IAEA 2004). Such discrepancies may be attributable to differences in algal species or metal complexation in different waters as well as to the inclusion of nonalgal particulate matter in earlier study samples.

This study provides some of the first unequivocal measurements of the trace-element composition of natural oceanic protists. The SXRF microprobe provides a direct measure of elemental composition, eliminating the need for stable or radioisotope additions, size fractionation, sequential acid leaches, or any other treatment that may lead to artifacts or obscure the composition of the plankton. The resulting cell quotas (normalized to either C, S, or P) are generally in good agreement with data from bulk analyses of natural assemblages, but they also identify differences in elemental composition for different types of cells that could not be detected with bulk analyses. Diatoms were enriched in Mn, Ni, and Zn relative to flagellates, and heterotrophs contained more P and Zn than autotrophs. Ratios of P to C were not constant during the Fe fertilization experiments, as cells became more enriched with P when they responded to the fertilizations. Cellular concentrations of Mn, Ni, and Zn also rose with fertilization in both patches, with greater increases in flagellates than in diatoms. The stoichiometric differences between similarly sized cell groups indicate that valuable information is lost when all types of co-occurring plankton are grouped together for analysis. SXRF reveals patterns that, while not completely understood at present, will allow us to better understand the linkage between lab-based culture work and field-based geochemical studies, while also providing grist for the development of new insights into metal cycling within intact plankton communities and into the

causes of variability in the elemental composition of different types of plankton cells.

References

- BERMAN-FRANK, I., J. T. CULLEN, Y. SHAKED, R. M. SHERRELL, AND P. G. FALKOWSKI. 2001. Iron availability, cellular iron quotas, and nitrogen fixation in *Trichodesmium*. *Limnol. Oceanogr.* **46**: 1249–1260.
- BOOTH, B. C. 1987. The use of autofluorescence for analyzing oceanic phytoplankton communities. *Bot. Mar.* **30**: 101–108.
- BRULAND, K. W., J. R. DONAT, AND D. A. HUTCHINS. 1991. Interactive influences of bioactive trace-metals on biological production in oceanic waters. *Limnol. Oceanogr.* **36**: 1555–1577.
- CHASE, Z., AND N. M. PRICE. 1997. Metabolic consequences of iron deficiency in heterotrophic marine protozoa. *Limnol. Oceanogr.* **42**: 1673–1684.
- COALE, K. H., AND OTHERS. 2004. Southern Ocean Iron Enrichment Experiment: Carbon cycling in high- and low-Si waters. *Science* **304**: 408–414.
- , AND OTHERS. 1996. A massive phytoplankton bloom induced by an ecosystem-scale iron fertilization experiment in the equatorial Pacific Ocean. *Nature* **383**: 495–501.
- COLLIER, R., AND J. EDMOND. 1984. The trace-element geochemistry of marine biogenic particulate matter. *Prog. Oceanogr.* **13**: 113–199.
- COOK, R. B., AND C. A. KELLY. 1992. Sulphur cycling and fluxes in temperate dimictic lakes, p. 145–188. *In* R. W. Howarth, J. W. B. Stewart, and M. V. Ivanov [eds.], Sulphur cycling on the continents. Wiley.
- CUHEL, R. L., AND J. B. WATERBURY. 1984. Biochemical composition and short term nutrient incorporation patterns in a unicellular marine cyanobacterium, *Synechococcus* (WH7803). *Limnol. Oceanogr.* **29**: 370–374.
- CULLEN, J. T., Z. CHASE, K. H. COALE, S. E. FITZWATER, AND R. M. SHERRELL. 2003. Effect of iron limitation on the cadmium to phosphorus ratio of natural phytoplankton assemblages from the Southern Ocean. *Limnol. Oceanogr.* **48**: 1079–1087.
- , T. W. LANE, F. M. M. MOREL, AND R. M. SHERRELL. 1999. Modulation of cadmium uptake in phytoplankton by seawater CO₂ concentration. *Nature* **402**: 165–167.
- DE BAAR, H. J. W., M. A. VAN LEEUWE, R. SCHAREK, L. GOEYENS, K. M. J. BAKKER, AND P. FRITSCH. 1997. Nutrient anomalies in *Fragilariopsis kerguelensis* blooms, iron deficiency and the nitrate/phosphate ratio (A. C. Redfield) of the Antarctic Ocean. *Deep-Sea Res. II* **44**: 229–260.
- DE LA ROCHA, C. L., D. A. HUTCHINS, M. A. BRZEZINSKI, AND Y. H. ZHANG. 2000. Effects of iron and zinc deficiency on elemental composition and silica production by diatoms. *Mar. Ecol. Prog. Ser.* **195**: 71–79.
- DONAT, J. R., AND K. W. BRULAND. 1995. Trace elements in the oceans, p. 247–281. *In* B. Salbu and E. Steinnes [eds.], Trace elements in natural waters. CRC.
- DORTCH, Q., T. L. ROBERTS, J. R. CLAYTON, JR., AND S. I. AHMED. 1983. RNA/DNA ratios and DNA concentrations as indicators of growth rate and biomass in planktonic marine organisms. *Mar. Ecol. Prog. Ser.* **13**: 61–71.
- FAN, C., P. M. GLIBERT, J. ALEXANDER, AND M. W. LOMAS. 2003. Characterization of urease activity in three marine phytoplankton species, *Aureococcus anophagefferens*, *Prorocentrum minimum*, and *Thalassiosira weissflogii*. *Mar. Biol.* **142**: 949–958.
- GEIDER, R. J., AND J. LA ROCHE. 2002. Redfield revisited: Variability of C:N:P in marine microalgae and its biochemical basis. *Eur. J. Phycol.* **37**: 1–17.
- GISSELSON, L.-A., E. GRANIELI, AND J. PALLON. 2001. Variation in cellular nutrient status within a population of *Dinophysis norvegica* (Dinophyceae) growing in situ: Single-cell elemental analysis by use of a nuclear microprobe. *Limnol. Oceanogr.* **46**: 1237–1242.
- GORDON, R. M., K. S. JOHNSON, AND K. H. COALE. 1998. The behaviour of iron and other trace elements during the IronEx-I and PlumEx experiments in the Equatorial Pacific. *Deep-Sea Res. II* **45**: 995–1041.
- GUNDERSEN, K., M. HELDAL, S. NORLAND, D. A. PURDIE, AND A. H. KNAP. 2002. Elemental C, N, and P cell content of individual bacteria collected at the Bermuda Atlantic Time-series Study (BATS) site. *Limnol. Oceanogr.* **47**: 1525–1530.
- HO, T. Y., A. QUIGG, Z. V. FINKEL, A. J. MILLIGAN, K. WYMAN, P. G. FALKOWSKI, AND F. M. M. MOREL. 2003. The elemental composition of some marine phytoplankton. *J. Phycol.* **39**: 1145–1159.
- HUTCHINS, D. A., AND K. W. BRULAND. 1998. Iron-limited diatom growth and Si:N uptake ratios in a coastal upwelling regime. *Nature* **393**: 561–564.
- , A. E. WITTER, A. BUTLER, AND G. W. LUTHER. 1999. Competition among marine phytoplankton for different chelated iron species. *Nature* **400**: 858–861.
- IAEA. 2004. Sediment distribution coefficients and concentration factors for biota in the marine environment. Tech. Rept. Ser. No. 422, International Atomic Energy Agency.
- LOSCHER, B. M. 1999. Relationships among Ni, Cu, Zn and major nutrients in the Southern Ocean. *Mar. Chem.* **67**: 67–102.
- MALDONADO, M. T., AND N. M. PRICE. 1999. Utilization of iron bound to strong organic ligands by plankton communities in the subarctic Pacific Ocean. *Deep-Sea Res. II* **46**: 2447–2473.
- MARTIN, J. H., K. W. BRULAND, AND W. W. BROENKOW. 1976. Cadmium transport in the California Current, p. 159–184. *In* H. Windom and R. Duce [eds.], Marine pollutant transfer. Heath.
- , AND G. A. KNAUER. 1973. The elemental composition of plankton. *Geochim. Cosmochim. Acta* **37**: 1639–1653.
- MENDEN-DEUER, S., AND E. J. LESSARD. 2000. Carbon to volume relationships for dinoflagellates, diatoms, and other protist plankton. *Limnol. Oceanogr.* **45**: 569–579.
- , ———, AND J. SATTERBERG. 2001. Effect of preservation on dinoflagellate and diatom cell volume and consequences for carbon biomass predictions. *Mar. Ecol. Prog. Ser.* **222**: 41–50.
- MENZEL, D. W., AND J. H. RYTHER. 1964. The composition of particulate organic matter in the western Atlantic Ocean. *Limnol. Oceanogr.* **9**: 179–186.
- MOAL, J., V. MARTIN-JEZEQUEL, R. P. HARRIS, J. F. SAMAIN, AND S. A. POULET. 1987. Interspecific and intraspecific variability of the chemical composition of marine phytoplankton. *Oceanol. Acta* **10**: 339–346.
- MONTAGNES, D. J. S., J. A. BERGES, P. J. HARRISON, AND F. J. R. TAYLOR. 1994. Estimating carbon, nitrogen, protein and chlorophyll *a* from volume in marine phytoplankton. *Limnol. Oceanogr.* **39**: 1044–1060.
- MOREL, F. M. M., AND R. J. M. HUDSON. 1985. The geobiological cycle of trace elements in aquatic systems: Redfield revisited, p. 251–281. *In* W. Stumm [ed.], Chemical processes in lakes. Wiley.
- , J. R. REINFELDER, S. B. ROBERTS, C. P. CHAMBERLAIN, J. G. LEE, AND D. YEE. 1994. Zinc and carbon co-limitation of marine phytoplankton. *Nature* **369**: 740–742.
- OLIVEIRA, L., AND N. J. ANTIA. 1986. Some observations on the urea-degrading enzyme of the diatom *Cyclotella cryptica* and the role of nickel in its production. *J. Plankton Res.* **8**: 235–242.
- PAKULSKI, J. D., R. B. COFFIN, C. A. KELLEY, S. L. HOLDER, R.

- DOWNER, P. AAS, M. M. LYONS, AND W. H. JEFFREY. 1996. Iron stimulation of Antarctic bacteria. *Science* **383**: 133–134.
- PAYNE, C. D., AND N. M. PRICE. 1999. Effects of cadmium toxicity on growth and elemental composition of marine phytoplankton. *J. Phycol.* **35**: 293–302.
- PEERS, G. S., A. J. MILLIGAN, AND P. J. HARRISON. 2000. Assay optimization and regulation of urease activity in two marine diatoms. *J. Phycol.* **36**: 523–528.
- PRICE, N. M., AND F. M. M. MOREL. 1990. Cadmium and cobalt substitution for zinc in a marine diatom. *Nature* **344**: 658–660.
- QUIGG, A., AND OTHERS. 2003. The evolutionary inheritance of elemental stoichiometry in marine phytoplankton. *Nature* **425**: 291–294.
- REDFIELD, A. C., B. H. KETCHUM, AND F. A. RICHARDS. 1963. The influence of organisms on the composition of sea-water, p. 26–77. In M. N. Hill [ed.], *The sea*. Interscience.
- RHEE, G.-Y. 1978. Effects of N:P atomic ratios and nitrate limitation on algal growth, cell composition and nitrate uptake. *Limnol. Oceanogr.* **23**: 10–25.
- SAITO, M. A., J. W. MOFFETT, S. W. CHISHOLM, AND J. B. WATERBURY. 2002. Cobalt limitation and uptake in *Prochlorococcus*. *Limnol. Oceanogr.* **47**: 1629–1636.
- STERNER, R. W., AND J. J. ELSER. 2002. *Ecological stoichiometry*. Princeton Univ. Press.
- STOECKER, D. K., AND J. M. CAPUZZO. 1990. Predation on protozoa: Its importance to zooplankton. *J. Plankton Res.* **12**: 891–908.
- STRATHMANN, R. R. 1967. Estimating the organic carbon content of phytoplankton from cell volume or plasma volume. *Limnol. Oceanogr.* **12**: 411–418.
- SUNDA, W. G., AND S. A. HUNTSMAN. 1995. Iron uptake and growth limitation in oceanic and coastal phytoplankton. *Mar. Chem.* **50**: 189–206.
- , AND ———. 1997. Interrelated influence of iron, light and cell size on marine phytoplankton growth. *Nature* **390**: 389–392.
- , AND ———. 1998. Interactions among Cu^{2+} , Zn^{2+} , and Mn^{2+} in controlling cellular Mn, Zn, and growth rate in the coastal alga *Chlamydomonas*. *Limnol. Oceanogr.* **43**: 1055–1064.
- SUTCLIFFE, W. H., JR. 1965. Growth estimates from ribonucleic acid content in some small organisms. *Limnol. Oceanogr.* **10S**: R253–258.
- TAKEDA, S. 1998. Influence of iron availability on nutrient consumption ratio of diatoms in oceanic waters. *Nature* **393**: 774–777.
- TWINING, B. S., AND OTHERS. 2003. Quantifying trace elements in individual aquatic protist cells with a synchrotron X-ray fluorescence microprobe. *Anal. Chem.* **75**: 3806–3816.
- , S. B. BAINES, N. S. FISHER, AND M. R. LANDRY. In press. Cellular iron contents of plankton during the Southern Ocean Iron Experiment (SOFEX). *Deep-Sea Res. I*.
- VERITY, P. G., C. Y. ROBERTSON, C. R. TRONZO, M. G. ANDREWS, J. R. NELSON, AND M. E. SIERACKI. 1992. Relationships between cell volume and carbon and nitrogen content of marine photosynthetic nanoplankton. *Limnol. Oceanogr.* **37**: 1434–1446.

Received: 8 January 2004

Accepted: 7 June 2004

Amended: 5 July 2004